

On the uncertainty principle of neural networks

Jun-Jie Zhang, Dong-Xiao Zhang, Jian-Nan Chen and Long-Gang Pang,

Abstract—Despite the successes in many fields, it is found that neural networks are vulnerability and difficult to be both accurate and robust (robust means that the prediction of the trained network stays unchanged for inputs with non-random perturbations introduced by adversarial attacks). Various empirical and analytic studies have suggested that there is more or less a trade-off between the accuracy and robustness of neural networks. If the trade-off is inherent, applications based on the neural networks are vulnerable with untrustworthy predictions. It is then essential to ask whether the trade-off is an inherent property or not. Here, we show that the accuracy-robustness trade-off is an intrinsic property whose underlying mechanism is deeply related to the uncertainty principle in quantum mechanics. We find that for a neural network to be both accurate and robust, it needs to resolve the features of the two conjugated parts x (the inputs) and Δ (the derivatives of the normalized loss function J with respect to x), respectively. Analogous to the position-momentum conjugation in quantum mechanics, we show that the inputs and their conjugates cannot be resolved by a neural network simultaneously.

Index Terms—explainable neural networks, accuracy robustness trade-off, adversarial attack, uncertainty principle, deep learning.

1 INTRODUCTION

A n intriguing issue concerning the deep neural networks has garnered significant attentions recently. Despite the wide applications in many fields, such as image classification [1], speech recognition [2], playing chess [3] and games [4], predicting protein structures [5], designing chips [6], searching for particles [7], and solving quantum systems [8], [9], etc., these well-trained models are found to be vulnerable under attacks that are imperceptible in terms of human sensations. Overwhelming empirical evidences have manifested that a small non-random perturbation can make a carefully designed neural network give erroneous predictions at a high coincidence [10], [11], [12], [13], [14], [15], [16], [17]. One of the widely used attacking examples is the Fast Gradient Stochastic Method [18] (FGSM), where the classification result of an input image can be easily altered by adding a small disturbance (Fig. 1).

Seeing the fact that more and more researchers are seeking to understand the neural networks, it is crucial for us to find the bottom line that we are able to explain them. Meanwhile, since many researchers are using neural networks to aid their investigations, it is also important for us to realize that if the neural networks are brittle to even small perturbations, applications based on the state-of-art deep learning will be under potential risks. For instance, scientific discoveries predicted by neural networks may be untrustworthy owing to small experimental errors; numerical neural network based PDE (Partial Differential Equations) solvers may yield acausal and counterfactual evolutions for a small distortion in the initial conditions, and medical diagnose can falsely discriminate the cancer cells due to disturbances that the doctors cannot tell by eyes, etc. Therefore, knowing the underlying reasons for this trade-off

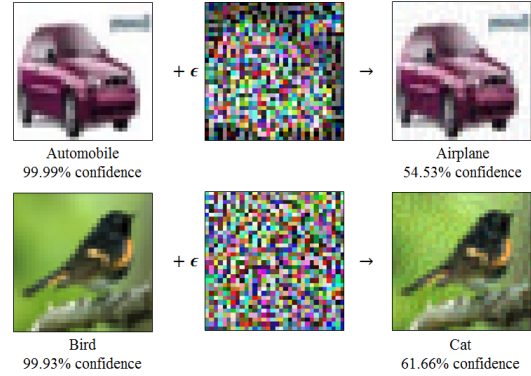


Fig. 1. FGSM attack reduces the test accuracy by adding an imperceptible non-random noise. The trained Googlenet (see the implementation used in this work in Ref. [19]) gives a 90.78% test accuracy on the test set and only 3.67% robust accuracy under the FGSM attack. The attack is achieved via the transformation $X_0 \rightarrow X_0 + \epsilon \text{sign}(\nabla_{Xj}(X_0 | X_0, Y_{\text{True}}, \theta))$, where X_0 denotes the input images to be transformed and classified, $\epsilon = 8/255$ and $\text{sign}(\nabla_{Xj}(X_0 | X_0, Y_{\text{True}}, \theta))$ gives the non-random noise with $j(X_0 | X_0, Y_{\text{True}}, \theta)$ denoting the loss function.

is of vital importance in understanding this phenomenon and further optimize the relevant applications to mitigate the influence of the attacks.

Intuitively, it is hard to understand the vulnerability phenomenon since the classical approximation theorems have already shown that a continuous function can be approximated arbitrarily well by a neural network [20], [21], [22], [23]—stable problems described by stable functions should always be solved stably in principle. Therefore, a natural question concerning this issue is to ask whether the trade-off between the accuracy and the robustness is an intrinsic and universal property of neural networks. If it is purely a matter of neural architecture design and training data acquisition, we only need to concentrate on the designing and training side. If, on the other hand, it involves some intrinsic properties which stand at the foundations

• *J. Zhang, D. Zhang and J. Chen are with the Division of Computational physics and Intelligent modeling, Northwest Institute of Nuclear Technology, Xi'an 710024, China*
E-mail: zjacob@mail.ustc.edu.cn

• *L. Pang is with the Key Laboratory of Quark & Lepton Physics of Ministry of Education, Central China Normal University, Wuhan 430079, China.*

of deep learning, we need to further study the trade-off in depth.

To understand the phenomenon, various empirical studies [15], [24], [25] involving different network structures, sizes, performances and even the scales of the training data, all suggest that there is more or less a trade-off between the accuracy and the robustness. Along with the experimental evidences, theoretical studies [18], [26], [27], [28] ranging from binary classification models to the information theory based analysis also support the possible trade-off in neural networks. Despite the fact that we still lack a proof to certify the uncertainty principle, many researchers have already begun the concurrent training strategy which optimizes both the robustness and the accuracy of deep neural networks [25], [27], [29], [30], [31], [32], [33], [34].

In this work, we have showed that the accuracy-robustness trade-off is mathematically equivalent to the uncertainty principle in quantum mechanics, where two complementary factors cannot be measured to an arbitrary high accuracy simultaneously. Similarly, we have demonstrated analytically and experimentally that two complementary quantities in neural networks cannot be resolved simultaneously. Our work reveals that only if one finds out the complementary features of a neural network, will they be able to conduct a concurrent training [30] to achieve a balance between the accuracy and robustness in the specific applications.

2 OBSERVATION FOR OBTAINING ACCURATE AND ROBUST NETWORKS

In image classification, a well-trained neural network separates the data points (images) into several classes. If the FGSM attack decreases the classification accuracy (as introduced above), it may be possible that we observe an increase in accuracy following the opposite direction of the FGSM attack.

In Fig. 3 we present the test and robust accuracies of the training set for two different network structures when we iteratively apply the opposite FGSM attack via

$$\begin{aligned} X_{n+1} &= X_n - \epsilon \text{sign}(\nabla_{Xj}(X_n | X_0, Y_{\text{True}}, \theta)) \\ &\equiv X_n + D_n, \end{aligned} \quad (1)$$

where X_n and X_{n+1} denote the images before and after the iteration, X_0 corresponds to the raw images, Y_{True} represents the corresponding labels for X_n , $j(X_n | X_0, Y_{\text{True}}, \theta)$ is the loss function for a specific classification network with parameter θ , and we choose the constant $\epsilon = 8/255$ for Cifar-10 [35] data-set in our study. Note that Eq. (1) can only be applied to the training set since it requires the knowledge of the label Y_{True} . For simplicity, we will refer to the process in Eq. (1) as Iterative FGSM Augmentation (IFA) since it increases both the test and robust accuracies of the training set (see details in Fig. 2). We can see from Fig. 3 that with the increase of the iteration times, both test accuracy (TA) and robust accuracy (RA) also increase.

The Iterative FGSM Augmentation (IFA) pipeline aims at training a neural network of high test and high robust accuracies following from the observation that an opposite

direction of the FGSM attack increases both the test and robust accuracies (Fig. 3). However, the increase of the accuracies in Fig. 3 requires the pre-known of the label Y_{True} , which is not viable for the test set. In order to apply Eq. (1) for an accuracy increase of the test set, we need to build a neural network which transforms the raw images X_0 to the accumulated gradients Δ_N . With such a Pix2Pix network, we can obtain the accumulated gradients Δ_N for any given X_0 . Once Δ_N is obtained, one can construct $X_N = X_0 + \Delta_N$ as the input to the classifier, and X_N has both high test and high robust accuracies in terms of the trained classifier. This conjecture is illustrated in Fig. 2.

In Fig. 4, we schematically depict the effects of both the FGSM attack and the IFA so as to understand the underlying reasons for the increase of accuracies in IFA. The shaded areas correspond to the domains of different image classes which are determined by the loss function $j(X_n | X_0, Y_{\text{True}}, \theta)$. The FGSM attack transforms the input images via $X_1 = X_n + \epsilon \text{sign}(\nabla_{Xj}(X_0 | X_0, Y_{\text{True}}, \theta))$, and shifts the data points that belong to a certain domain towards other domains so as to attack the classification network. On the contrary, if we iteratively apply the FGSM attack in the opposite direction, we can move these data points back to their TRUE domain classes—thus gaining an augmentation of both the test and robust accuracies for the training set [18], [37].

For convenience, we introduce a new term

$$\begin{aligned} \Delta_N &\equiv X_N - X_0 \\ &= X_{N-1} + D_{N-1} - X_0 = \dots = \sum_{n=0}^{N-1} D_n, \end{aligned} \quad (2)$$

where N represents the final iteration number in IFA. As long as one can find Δ_N with given X_0 , (following Eq. (2)) they can contrast the image X_N , which has both high test and robust accuracies. Therefore, for a neural network that is both accurate and robust can capture the features of both X_0 and Δ_N . However, as will be shortly revealed, due to the uncertainty principle of neural networks, such a neural network cannot be designed and trained.

3 DERIVATION OF THE UNCERTAINTY PRINCIPLE OF NEURAL NETWORKS

In the year 1927, Heisenberg introduced the first formulation of the uncertainty principle in his German article [38] that the “imprecisions” of simultaneously measuring the position q and momentum p of the electron is limited by the relation $\delta p \delta q \sim h$, where h is the Planck’s constant. Using his matrix mechanics, he postulated that the matrices Q and P representing the canonical position and momentum variables of a particle satisfy the so-called canonical commutation,

$$[Q, P] \equiv QP - PQ = \frac{h}{2\pi}. \quad (3)$$

The non-commutative property of matrices Q and P plays a central role in Heisenberg’s uncertainty principle, which can be understood in term of Niels Bohr’s complementarity principle [39]. In short, as one of the most famous aspects of quantum mechanics, the uncertainty principle simply states that one cannot assign exact simultaneous values to the position and momentum of a physical system.

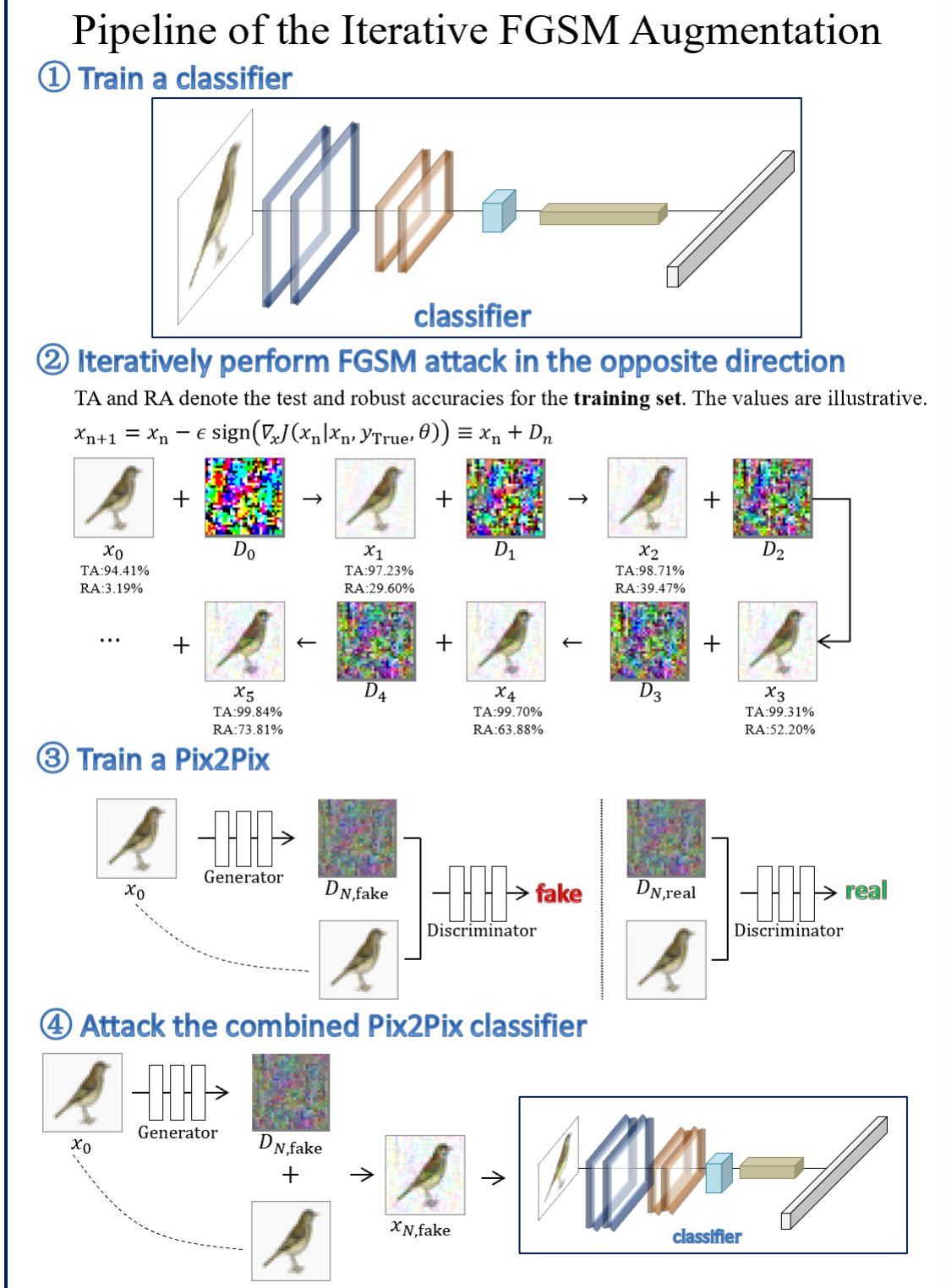


Fig. 2. The pipeline of the iterative FGSM augmentation. ① A classifier (for instance the Residual neural network) $j(X_n | X_0, Y_{\text{True}}, \theta)$ is first trained, where X_0 and Y_{True} denote the raw images and labels. ② Based on the observation that the opposite direction of the FGSM attack increases the accuracy, we iteratively perform the FGSM attack in the opposite direction so as to increase the test accuracies (TA) and robust accuracies (RA) of the training set. Hence, as long as one obtains Δ_N for image X_0 , the addition $X_0 + \Delta_N$ will produce both high TA and high RA. ③ For the test set, since the label Y_{True} is unknown, Δ_N cannot be obtained directly. Instead, we train a Pix2Pix network that captures the features of the map $X_0 \rightarrow \Delta_N$. ④ Providing the images X_0 (in the test set) to the Pix2Pix generator, we gain the conjugation Δ_N . Then, the iterative FGSM attack (with step size 4 and l_∞ loss) is applied to attack the combined neural network (Pix2Pix+classifier).

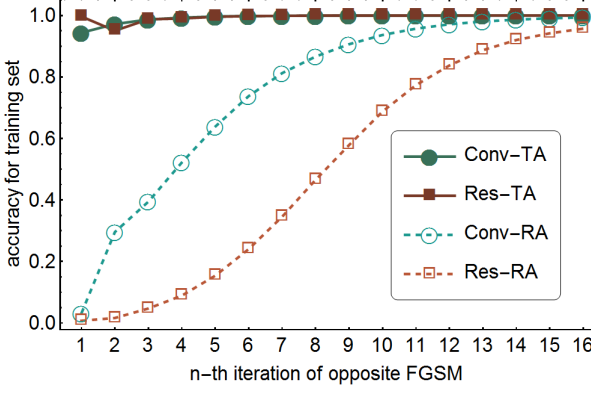


Fig. 3. Test accuracy (TA) and robust accuracy (RA) for training set. Two classifiers, the Convolutional (Conv) and Residual (Res) neural networks, are used to perform the opposite FGSM transformation following Eq. (1). The robust accuracy here refers to the accuracy when the input images are attacked via the iterative FGSM attack [36] with step size 4 and ℓ_∞ loss.

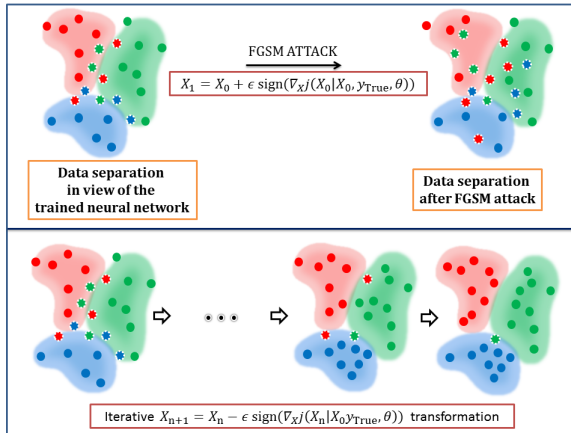


Fig. 4. Illustrative effect of the FGSM attack and the iterative FGSM augmentation (IFA). The shaded areas represent the domains of different classes determined by the classifiers. The upper panel: FGSM attack transforms some of the images (data points) that belong to a certain domain towards other domains, leading to a decrease of the accuracy. The lower panel: the iterative FGSM augmentation transforms the images towards the domains with correct classification, leading to an increase of the accuracy.

Here we adopt the symbols used in quantum theory. An operator is a mathematical rule that transforms a given function into another. For example, if an input image is represented by the variable $X = (x_1, \dots, x_i, \dots, x_M)$ with $x_1, \dots, x_i, \dots, x_M$ denoting the pixels, we can define the operator \hat{x}_i corresponds to the eigenvalue x_i as

$$\hat{x}_i J(X|X_0, Y_{\text{True}}, \theta) = x_i J(X|X_0, Y_{\text{True}}, \theta), \quad (4)$$

where for a given image class with label Y_{True} , the trained loss function $J(X|X_0, Y_{\text{True}}, \theta)$ can be seen as a wave function if we normalize it to unity, $\int J(X|X_0, Y_{\text{True}}, \theta)^2 = 1$. The M -dimensional function $J(X|X_0, Y_{\text{True}}, \theta)$ is known as the eigenvector of operator x_i . In the construction of a neural net, a set of weights $\theta = \{\theta_1, \theta_2, \dots, \theta_N\}$ are introduced. The weights are trained with the input-label pairs $\{X, Y_{\text{True}} \in \{\text{Training set}\}\}$ such that the loss function $J(X|X_0, Y_{\text{True}}, \theta)$ takes its minimum. For convenience, we

also introduce another operator \hat{p}_i defined as

$$\hat{p}_i J(X|X_0, Y_{\text{True}}, \theta) = \frac{\partial}{\partial x_i} J(X|X_0, Y_{\text{True}}, \theta). \quad (5)$$

Operator \hat{p}_i resembles the operation of the attack, since it is reported that even without the “Sign” of the FGSM a successful attack can also be achieved [37]. All operators introduced here are real, which are different from the ones in quantum theory.

The average value of an operator \hat{A} on function $J(X|X_0, Y_{\text{True}}, \theta)$ takes the following form,

$$\langle \hat{A} \rangle = \int J(X|X_0, Y_{\text{True}}, \theta) \hat{A} J(X|X_0, Y_{\text{True}}, \theta) dX, \quad (6)$$

where the bracket $\langle \cdot \rangle$ is the Dirac symbol widely used in physics.

In general, for any two unbounded real operators $\langle \hat{A} \rangle$ and $\langle \hat{B} \rangle$, the following relation holds

$$0 \leq \langle (\hat{A} - i\hat{B})^* (\hat{A} - i\hat{B}) \rangle = \langle \hat{A}^2 \rangle - i\langle \hat{A}^* \hat{B} - \hat{B}^* \hat{A} \rangle + \langle \hat{B}^2 \rangle. \quad (7)$$

If we use the property $\langle \hat{A}^2 \rangle + \langle \hat{B}^2 \rangle \leq 2\langle \hat{A}^2 \rangle^{1/2}\langle \hat{B}^2 \rangle^{1/2}$, we can obtain the basic bound for the commutator $[\hat{A}, \hat{B}] \equiv \hat{A}\hat{B} - \hat{B}\hat{A}$,

$$|i\frac{1}{2}\langle [\hat{A}, \hat{B}] \rangle| \leq \langle \hat{A}^2 \rangle^{\frac{1}{2}} \langle \hat{B}^2 \rangle^{\frac{1}{2}}. \quad (8)$$

For simplicity, we further assume that the average value of operators $\langle \hat{A} \rangle$ and $\langle \hat{B} \rangle$ are both zero, i.e.,

$$\langle \hat{A} \rangle = \int J(X|X_0, Y_{\text{True}}, \theta) \hat{A} J(X|X_0, Y_{\text{True}}, \theta) dX = 0, \quad (9)$$

and

$$\langle \hat{B} \rangle = \int J(X|X_0, Y_{\text{True}}, \theta) \hat{B} J(X|X_0, Y_{\text{True}}, \theta) dX = 0. \quad (10)$$

Therefore, the standard deviations for eigenvalues a and b with respect to \hat{A} and \hat{B} reads,

$$\sigma_a \sigma_b = \langle \hat{A}^2 - \langle \hat{A} \rangle^2 \rangle^{\frac{1}{2}} \langle \hat{B}^2 - \langle \hat{B} \rangle^2 \rangle^{\frac{1}{2}} = \langle \hat{A}^2 \rangle^{\frac{1}{2}} \langle \hat{B}^2 \rangle^{\frac{1}{2}}. \quad (11)$$

In terms of the neural networks, we can simply replace operators \hat{A} and \hat{B} by \hat{p}_i and \hat{x}_i introduced in Eq. (14) and (15), and this leads to the uncertainty relation

$$\begin{aligned} \sigma_{\hat{p}_i} \sigma_{\hat{x}_i} &\geq |i\frac{1}{2}\langle [\hat{p}_i, \hat{x}_i] \rangle| \\ &= \frac{1}{2}|i\int J(X|X_0, Y_{\text{True}}, \theta)^2 dX| \\ &= \frac{1}{2}, \end{aligned} \quad (12)$$

where we have used the relation

$$\begin{aligned} [\hat{p}_i, \hat{x}_i] J(X|X_0, Y_{\text{True}}, \theta) &= [\hat{p}_i \hat{x}_i - \hat{x}_i \hat{p}_i] J(X|X_0, Y_{\text{True}}, \theta) \\ &= J(X|X_0, Y_{\text{True}}, \theta). \end{aligned} \quad (13)$$

Note that Eq. (16) is a general result for all neural networks.

4 ACCURACY-ROBUSTNESS TRADE-OFF IN VIEW OF THE UNCERTAINTY PRINCIPLE IN QUANTUM MECHANICS

Here we adopt the symbols used in quantum theory. An operator is a mathematical rule that transforms a given function into another. For example, if an input image is represented by the variable $X = (x_1, \dots, x_i, \dots, x_M)$ with $x_1, \dots, x_i, \dots, x_M$ denoting the pixels, we can define the operator \hat{x}_i corresponds to the eigenvalue x_i as

$$\hat{x}_i J(X|X_0, Y_{\text{True}}, \theta) = x_i J(X|X_0, Y_{\text{True}}, \theta), \quad (14)$$

where for a given image class with label Y_{True} , the trained loss function $J(X|X_0, Y_{\text{True}}, \theta)$ can be seen as a wave function if we normalize it to unity, $\int J(X|X_0, Y_{\text{True}}, \theta)^2 = 1$. The M -dimensional function $J(X|X_0, Y_{\text{True}}, \theta)$ is known as the eigenvector of operator x_i . In the construction of a neural net, a set of weights $\theta = \{\theta_1, \theta_2, \dots, \theta_N\}$ are introduced. The weights are trained with the input-label pairs $\{X, Y_{\text{True}} \in \{\text{Training set}\}\}$ such that the loss function $J(X|X_0, Y_{\text{True}}, \theta)$ takes its minimum. For convenience, we also introduce another operator \hat{p}_i defined as

$$\hat{p}_i J(X|X_0, Y_{\text{True}}, \theta) = \frac{\partial}{\partial x_i} J(X|X_0, Y_{\text{True}}, \theta). \quad (15)$$

Operator \hat{p}_i resembles the operation of the attack, since it is reported that even without the “Sign” of the FGSM a successful attack can also be achieved [37]. All operators introduced here are real, which are different from the ones in quantum theory.

In terms of the neural networks, we have the uncertainty relation (see derivation in Methods)

$$\sigma_{\hat{p}_i} \sigma_{\hat{x}_i} \geq \frac{1}{2}, \quad (16)$$

To understand how Eq. (16) leads to the trade-off of accuracy and robustness, we consider an example of a binary classifier which distinguishes the Mesons and the Baryons. In Fig. 5, we schematically plot the normalized loss functions $J(X|X_0, Y_{\text{True,Mesons}}, \theta)$ and $J(X|X_0, Y_{\text{True,Baryons}}, \theta)$ and their corresponding conjugations. The particle data can be seen as vectors in the high dimensional space Ω . A classifier $J(X|X_0, Y_{\text{True,Mesons}}, \theta)$ maps all data points to a scalar value. For the points that correspond to the Mesons, function $J(X|X_0, Y_{\text{True,Mesons}}, \theta)$ assigns a larger probability value than those for the Baryons. For Mesons, a higher test accuracy is expected if the standard deviation $\sigma_{X, \text{Mesons}}$ of $J(X|X_0, Y_{\text{True,Mesons}}, \theta)$ is smaller. Accordingly, a higher robust accuracy, which corresponds to the conjugation $\tilde{J}(\Delta_N|X_0, Y_{\text{True,Mesons}}, \theta)$, requires a smaller standard deviation $\sigma_{\Delta_N, \text{Mesons}}$. Since

$$\begin{aligned} \Delta_N &= \sum_{n=0}^{N-1} D_n \sim \sum_{n=0}^{N-1} J(X_n|X_0, Y_{\text{True,Mesons}}, \theta) \\ &= \sum_{n=0}^{N-1} \hat{P} J(X_n|X_0, Y_{\text{True,Mesons}}, \theta), \end{aligned} \quad (17)$$

for the simplest case, we can choose $N = 1$, and thus, we obtain $\Delta_{N=1} = \hat{P} J(X_0|X_0, Y_{\text{True,Mesons}}, \theta)$ and $\sigma_{\Delta_1, \text{Mesons}} =$

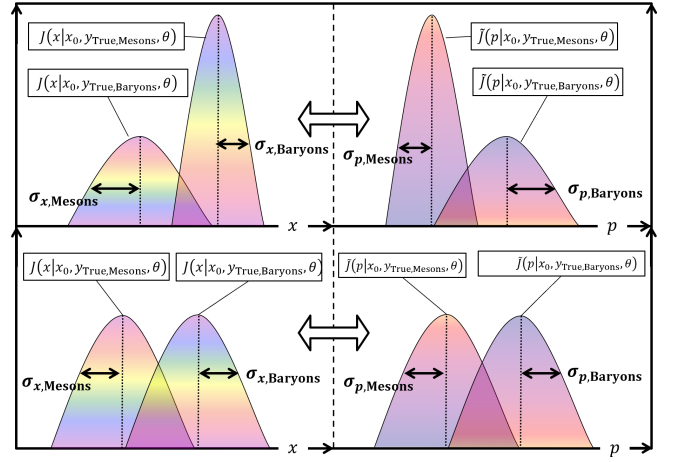


Fig. 5. Schematic illustration of the uncertain relation in binary classification. $J(X|X_0, Y_{\text{True,Mesons}}, \theta)$ and $J(X|X_0, Y_{\text{True,Baryons}}, \theta)$ denote the normalized loss functions; $\tilde{J}(P|X_0, Y_{\text{True,Mesons}}, \theta)$ and $\tilde{J}(P|X_0, Y_{\text{True,Baryons}}, \theta)$ denote the corresponding conjugations.

$\sigma_{P, \text{Mesons}}$. Following from the uncertainty relation (17), we have

$$\sigma_{p_i, \text{Mesons}} \sigma_{x_i, \text{Mesons}} \geq \frac{1}{2}. \quad (18)$$

We see that one cannot build such a neural network $J(X|X_0, Y_{\text{True,Mesons}}, \theta)$ that $\sigma_{X, \text{Mesons}}$ and $\sigma_{P, \text{Mesons}}$ are simultaneously small. For cases where $N > 1$, the analogy also holds, rather a more complex mathematics needs to be performed.

5 FAILURE OF CONSTRUCTING A NEURAL NETWORK OF BOTH HIGH TEST AND HIGH ROBUST ACCURACIES

The uncertainty relation in Eq. (16) can be manifested in various forms. Here, as an example, we will perceive the trade-off in terms of building a neural network that transforms X_0 to Δ_N . From Fig. 3, we know that if such a neural network can be designed and trained, we can simply use $X_N = X_0 + \Delta_N$ to achieve both high TA and RA. However, as we will shortly demonstrate training such a network involves certain subtleties practically.

We start with a Pix2Pix network [19] (which maps an image to another) with training sample pairs (X_0, Δ_N) , where the target Δ_N is generated iteratively using Eq. (1) and (2) with $N = 200$ (see details in Fig. 2). Ahead of the generation of Δ_N , two classifiers, the Convolutional (ConvNet) and the Residual (ResNet) networks are trained for the Cifar-10 data-set at epoch number $N_{\text{epoch}} = 1, 5, 50$ respectively. The values of the training epoch affect the accuracies of the classifiers. The trained Pix2Pix produces Δ_N , which are used to construct images $X_N = X_0 + \Delta_N$. The TA and RA of the combined classifiers Pix2Pix+ConvNet/ResNet on X_N manifest the trade-off: TA and RA cannot be both high for larger epoch numbers N_{epoch} (Fig. 6).

Fig. 6 gives the TA and RA of these classifiers. The following conclusions can be drawn accordingly:

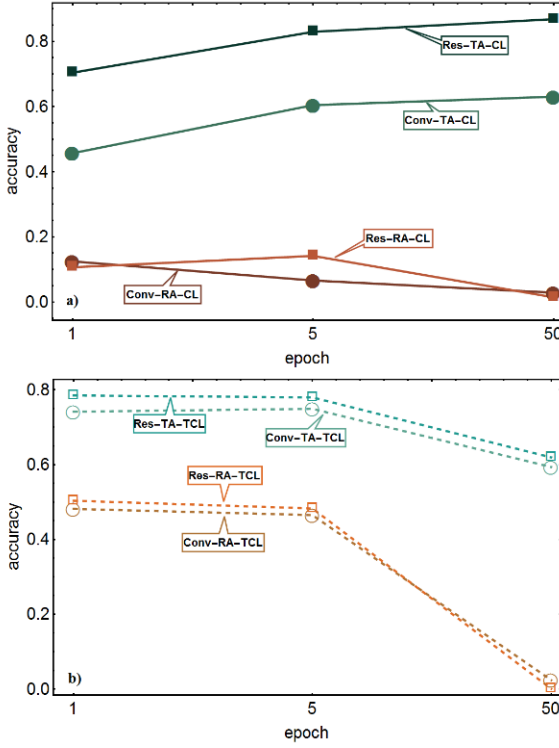


Fig. 6. Test and robust accuracies of the classifiers. Res and Conv correspond to the Residual and convolutional networks. TA and RA represent the test and robust accuracies. CL stands for classifiers that are not combined with a Pix2Pix network and TCL stands for the transformed classifiers (i.e., Pix2Pix+Res/Conv). The attack is performed via the iterative FGSM [36] with 4 steps and l_∞ loss. All TCLs are in dashed lines and CLs are in solid lines.

- For the classifiers (Conv/Res), an increase in TA corresponds to a decrease in RA in general (Fig. 6 (a)), indicating that there is a trade-off between TA and RA.
- For the combined classifiers (Pix2Pix+Conv/Res), TA and RA both decrease (Fig. 6 (b)) with the increasing of the epoch number N_{epoch} , indicating that the IFA pipeline fails at increasing TA and RA simultaneously.

The results presented in Fig. 6 can be understood from the frequency-principle [40] (F-Principle) in a straightforward way. It is proposed by the F-Principle that “the DNNs tend to fit training data by a low-frequency function resulting from the smoothness/regularity of the commonly used activation functions”. Therefore, it is harder for the neural networks to predict high-frequency images than the low-frequency ones. To be specific, in the training of reducing the loss function $j(\theta|X_0, Y_{\text{True}})$, smaller values of j indicate higher training (and also test) accuracies if the network is not over fitted. For a network to distinguish among the many classes, high-frequency features are gradually resolved in the training course. Thus, a neural network with higher accuracy contains more high-frequency features [41], [42]. In Fig. 7, we compare the test accuracies of the classifiers with the proportion of the high frequencies of the generated Δ_1 . We see that Δ_1 contains more high frequency components with the increasing of the test accuracies, making it more difficult for a Pix2Pix network to produce.

Therefore, a more accurate classifier generates the

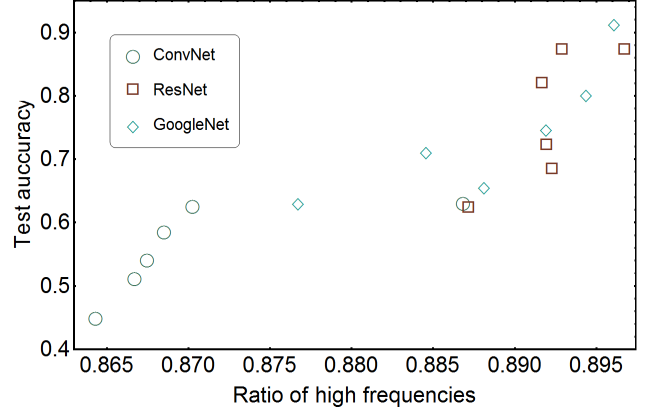


Fig. 7. Ratio of high frequencies is roughly proportional to the test accuracies. Ratio of high frequencies is obtained via the formula $(|\text{FFT}[\Delta_1]| - |\text{FFT}[\Delta_1]_{\text{LF}}|)/|\text{FFT}[\Delta_1]|$, where $|\text{FFT}[\Delta_1]|$ takes the slices of $[5 : 26, 5 : 26, 1]$ in $|\text{FFT}[\Delta_1]|$. The three networks are trained for epochs 1, 2, 3, 5, 10, and 50 to gain the different test accuracies.

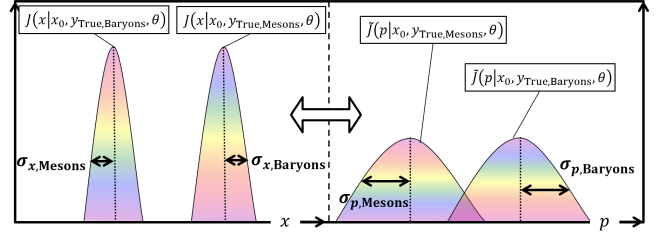


Fig. 8. Illustration of the uncertainty principle when the two classes are separated far apart. Left panel: the two classes can be distinguished far apart. Right panel: the corresponding conjugations can overlap.

difference Δ_1 of higher frequencies; and a more robust classifier corresponds to the generation (by Pix2Pix) of Δ_1 , which is harder to resolve if Δ_1 contains more high frequency components. This is the reason that both TA and RA decrease at $N_{\text{epoch}} = 50$. In addition, if the classifier is of low accuracy initially, we can increase both its TA and RA, as shown by the case of $N_{\text{epoch}} = 1$ in Fig. 6.

6 CONCLUSION

One natural question often raised is that if we can train a network such that different classes are far apart (the left panel of Fig. 8), the network must be robust enough that any small attacks should have minor affects on the robust accuracy. However, classification is not purely a matter of the separation of different domains, rather it reflects the sort of information that we perceive in terms of a certain view. For a trained network, if two classes can be separated far apart in view of the input images (so the network is smooth and robust as defined in Ref [43]), their corresponding σ_X should be small, which inevitably leads to large σ_{Δ_N} . If, on the other hand, we classify the images in view of the conjugation Δ_N , the two classes can overlap due to the large σ_{Δ_N} (the right panel of Fig. 8). Intuitively, when Δ_N is added on X , $X + \Delta_N$ can overlap in terms of the conjugation (normalized) loss \tilde{J} .

In conclusion, we find that for a classifier to be both accurate and robust, it needs to resolve the features of

both the input X_0 and its conjugate $\nabla_X j(X_n | X_0, Y_{\text{True}}, \theta)$, which is restricted by the uncertainty relation Eq. (16). The underlying mathematics of the uncertainty principle for neural networks is equivalent to that used in the quantum theory, indicating that the uncertainty relation is an intrinsic property for neural networks. Our work suggests that more work should be conducted in specific fields so as to dig out the complementary features for concurrent training. Meanwhile, more attentions should be paid to the vulnerability of neural networks in case of the day when this issue has widely exposed due to the growing needs in the application of neural networks.

ACKNOWLEDGMENTS

We thank Prof. David Donoho from Stanford University for providing valuable suggestions on the accuracy robustness of neural networks. Many thanks are given to Prof. Tai-Jiao Du, Prof. Hai-Yan xie, Prof. Yin-Jun Gao and Prof. Guo-Liang Peng from Northwest Institute of Nuclear Technology for their funding and support of the work. The work is partly supported by the National Science Foundation of China (NSFC) under the grant number 12105227.

REFERENCES

- [1] A. Krizhevsky, I. Sutskever, and G. E. Hinton, "Imagenet classification with deep convolutional neural networks," *Commun. ACM*, vol. 60, no. 6, p. 84–90, may 2017. [Online]. Available: <https://doi.org/10.1145/3065386>
- [2] G. Hinton, L. Deng, D. Yu, G. E. Dahl, A.-r. Mohamed, N. Jaitly, A. Senior, V. Vanhoucke, P. Nguyen, T. N. Sainath, and B. Kingsbury, "Deep neural networks for acoustic modeling in speech recognition: The shared views of four research groups," *IEEE Signal Processing Magazine*, vol. 29, no. 6, pp. 82–97, 2012.
- [3] D. Silver, A. Huang, C. J. Maddison, A. Guez, L. Sifre, G. van den Driessche, J. Schrittwieser, I. Antonoglou, V. Panneershelvam, M. Lanctot, S. Dieleman, D. Grewe, J. Nham, N. Kalchbrenner, I. Sutskever, T. Lillicrap, M. Leach, K. Kavukcuoglu, T. Graepel, and D. Hassabis, "Mastering the game of go with deep neural networks and tree search," *Nature*, vol. 529, no. 7587, pp. 484–489, jan 2016.
- [4] J. Schrittwieser, I. Antonoglou, T. Hubert, K. Simonyan, L. Sifre, S. Schmitt, A. Guez, E. Lockhart, D. Hassabis, T. Graepel, T. Lillicrap, and D. Silver, "Mastering atari, go, chess and shogi by planning with a learned model," *Nature*, vol. 588, no. 7839, pp. 604–609, dec 2020.
- [5] A. W. Senior, R. Evans, J. Jumper, J. Kirkpatrick, L. Sifre, T. Green, C. Qin, A. Žídek, A. W. R. Nelson, A. Bridgland, H. Penedones, S. Petersen, K. Simonyan, S. Crossan, P. Kohli, D. T. Jones, D. Silver, K. Kavukcuoglu, and D. Hassabis, "Improved protein structure prediction using potentials from deep learning," *Nature*, vol. 577, no. 7792, pp. 706–710, jan 2020.
- [6] A. Mirhoseini, A. Goldie, M. Yazgan, J. W. Jiang, E. Songhori, S. Wang, Y.-J. Lee, E. Johnson, O. Pathak, A. Nazi, J. Pak, A. Tong, K. Srinivasa, W. Hang, E. Tuncer, Q. V. Le, J. Laudon, R. Ho, R. Carpenter, and J. Dean, "A graph placement methodology for fast chip design," *Nature*, vol. 594, no. 7862, pp. 207–212, jun 2021.
- [7] P. Baldi, P. Sadowski, and D. Whiteson, "Searching for exotic particles in high-energy physics with deep learning," *Nature Communications*, vol. 5, no. 1, jul 2014.
- [8] G. Carleo and M. Troyer, "Solving the quantum many-body problem with artificial neural networks," *Science*, vol. 355, no. 6325, pp. 602–606, 2017. [Online]. Available: <https://www.science.org/doi/abs/10.1126/science.aag2302>
- [9] L.-G. Pang, K. Zhou, N. Su, H. Petersen, H. Stöcker, and X.-N. Wang, "An equation-of-state-meter of quantum chromodynamics transition from deep learning," *Nature Communications*, vol. 9, no. 1, jan 2018.
- [10] C. Szegedy, W. Zaremba, I. Sutskever, J. Bruna, D. Erhan, I. Goodfellow, and R. Fergus, "Intriguing properties of neural networks," Jan. 2014, 2nd International Conference on Learning Representations, ICLR 2014 ; Conference date: 14-04-2014 Through 16-04-2014.
- [11] K. Eykholt, I. Evtimov, E. Fernandes, B. Li, A. Rahmati, C. Xiao, A. Prakash, T. Kohno, and D. Song, "Robust physical-world attacks on deep learning visual classification," in *2018 IEEE/CVF Conference on Computer Vision and Pattern Recognition*, 2018, pp. 1625–1634.
- [12] R. Jia and P. Liang, "Adversarial examples for evaluating reading comprehension systems," in *Proceedings of the 2017 Conference on Empirical Methods in Natural Language Processing*. Copenhagen, Denmark: Association for Computational Linguistics, Sep. 2017, pp. 2021–2031. [Online]. Available: <https://aclanthology.org/D17-1215>
- [13] H. Chen, H. Zhang, P.-Y. Chen, J. Yi, and C.-J. Hsieh, "Attacking visual language grounding with adversarial examples: A case study on neural image captioning," *PROCEEDINGS OF THE 56TH ANNUAL MEETING OF THE ASSOCIATION FOR COMPUTATIONAL LINGUISTICS (ACL)*, VOL 1, pp. 2587–2597, 2018.
- [14] N. Carlini and A. D. Wagner, "Audio adversarial examples: Targeted attacks on speech-to-text," *2018 IEEE SYMPOSIUM ON SECURITY AND PRIVACY WORKSHOPS (SPW 2018)*, pp. 1–7, 2018.
- [15] H. Xu, C. Caramanis, and S. Mannor, "Sparse algorithms are not stable: A no-free-lunch theorem," *IEEE Trans. Pattern Anal. Mach. Intell.*, pp. 187–193, 2012.
- [16] P. Benz, C. Zhang, A. Karjauv, and I. S. Kweon, "Robustness may be at odds with fairness: An empirical study on class-wise accuracy," in *NeurIPS 2020 Workshop on Pre-registration in Machine Learning*, ser. Proceedings of Machine Learning Research, L. Bertinetto, J. F. Henriques, S. Albanie, M. Paganini, and G. Varol, Eds., vol. 148. PMLR, 11 Dec 2021, pp. 325–342. [Online]. Available: <https://proceedings.mlr.press/v148/benz21a.html>
- [17] S. A. Morcos, G. T. D. Barrett, C. N. Rabinowitz, and M. Botvinick, "On the importance of single directions for generalization," *International Conference on Learning Representations*, 2018.
- [18] J. I. Goodfellow, J. Shlens, and C. Szegedy, "Explaining and harnessing adversarial examples," *international conference on learning representations*, 2015.
- [19] J.-J. Zhang, D.-X. Zhang, J.-N. Chen, and L.-G. Pang, "Robust and Test accuracy of the IFA pipeline and the frequencies related," 2021. [Online]. Available: <https://doi.org/10.7910/DVN/FKFJZQ>
- [20] G. Cybendo, "Approximations by superpositions of a sigmoidal function," *Mathematics of Control, Signals and Systems*, pp. 303–314, 1992.
- [21] K. Hornik, M. Stinchcombe, and H. White, "Multilayer feedforward networks are universal approximators," *Neural Networks*, vol. 2, no. 5, pp. 359–366, 1989. [Online]. Available: <https://www.sciencedirect.com/science/article/pii/0893608089900208>
- [22] E. Gelenbe, "Random Neural Networks with Negative and Positive Signals and Product Form Solution," *Neural Computation*, vol. 1, no. 4, pp. 502–510, 12 1989. [Online]. Available: <https://doi.org/10.1162/neco.1989.1.4.502>
- [23] E. Gelenbe, Z.-H. Mao, and Y.-D. Li, "Function approximation with spiked random networks," *IEEE Transactions on Neural Networks*, vol. 10, no. 1, pp. 3–9, Jan 1999.
- [24] D. Su, H. Zhang, H. Chen, J. Yi, P.-Y. Chen, and Y. Gao, "Is robustness the cost of accuracy? – a comprehensive study on the robustness of 18 deep image classification models," in *Computer Vision – ECCV 2018*, V. Ferrari, M. Hebert, C. Sminchisescu, and Y. Weiss, Eds. Cham: Springer International Publishing, 2018, pp. 644–661.
- [25] P. Arcaini, A. Bombarda, S. Bonfanti, and A. Gargantini, "Roby: a tool for robustness analysis of neural network classifiers," *2021 14th IEEE Conference on Software Testing, Verification and Validation (ICST)*, pp. 442–447, 2021.
- [26] H. Zhang, Y. Yu, J. Jiao, E. Xing, L. E. Ghaoui, and M. Jordan, "Theoretically principled trade-off between robustness and accuracy," in *Proceedings of the 36th International Conference on Machine Learning*, ser. Proceedings of Machine Learning Research, K. Chaudhuri and R. Salakhutdinov, Eds., vol. 97. PMLR, 09–15 Jun 2019, pp. 7472–7482. [Online]. Available: <https://proceedings.mlr.press/v97/zhang19p.html>

- [27] D. Tsipras, S. Santurkar, L. Engstrom, A. Turner, and A. Madry, "Robustness may be at odds with accuracy," *international conference on learning representations*, 2019.
- [28] V. Antun, J. M. Colbrook, and C. A. Hansen, "Can stable and accurate neural networks be computed? – on the barriers of deep learning and smale's 18th problem," 2021.
- [29] Y.-Y. Yang, C. Rashtchian, H. Zhang, R. R. Salakhutdinov, and K. Chaudhuri, "A closer look at accuracy vs. robustness," in *Advances in Neural Information Processing Systems*, H. Larochelle, M. Ranzato, R. Hadsell, M. F. Balcan, and H. Lin, Eds., vol. 33. Curran Associates, Inc., 2020, pp. 8588–8601. [Online]. Available: <https://proceedings.neurips.cc/paper/2020/file/61d77652c97ef636343742fc3dcf3ba9-Paper.pdf>
- [30] E. Arani, F. Sarfraz, and B. Zonooz, "Adversarial concurrent training: Optimizing robustness and accuracy trade-off of deep neural networks," *The British Machine Vision Conference (BMVC)*, 2020.
- [31] V. Sehwag, S. Mahloujifar, T. Handina, S. Dai, C. Xiang, M. Chiang, and P. Mittal, "Improving adversarial robustness using proxy distributions," 2021.
- [32] K. Leino, Z. Wang, and M. Fredrikson, "Globally-robust neural networks," *INTERNATIONAL CONFERENCE ON MACHINE LEARNING*, VOL 139, pp. 6212–6222, 2021.
- [33] V. Antun, F. Renna, C. Poon, B. Adcock, and C. A. Hansen, "On instabilities of deep learning in image reconstruction and the potential costs of ai," *PROCEEDINGS OF THE NATIONAL ACADEMY OF SCIENCES OF THE UNITED STATES OF AMERICA*, pp. 30 088–30 095, 2020.
- [34] A. Rozsa, M. Günther, and E. T. Boult, "Are accuracy and robustness correlated?" *2016 15TH IEEE INTERNATIONAL CONFERENCE ON MACHINE LEARNING AND APPLICATIONS (ICMLA 2016)*, pp. 227–232, 2016.
- [35] A. Krizhevsky, "Learning multiple layers of features from tiny images," 2009.
- [36] A. Kurakin, J. I. Goodfellow, and S. Bengio, "Adversarial examples in the physical world," *international conference on learning representations*, 2017.
- [37] A. Agarwal, R. Singh, and M. Vatsa, "The role of 'sign' and 'direction' of gradient on the performance of cnn," *CVPR Workshops*, pp. 2748–2756, 2020.
- [38] W. Heisenberg, "Über den anschaulichen inhalt der quantentheoretischen kinematik und mechanik," *Zeitschrift für Physik*, vol. 43, no. 3-4, pp. 172–198, mar 1927.
- [39] N. Bohr, "On the notions of causality and complementarity," *Science*, vol. 111, no. 2873, pp. 51–54, jan 1950.
- [40] J. Z.-Q. Xu, Y. Zhang, T. Luo, Y. Xiao, and Z. Ma, "Frequency principle: Fourier analysis sheds light on deep neural networks," *COMMUNICATIONS IN COMPUTATIONAL PHYSICS*, pp. 1746–1767, 2020.
- [41] J. Z.-Q. Xu, Y. Zhang, and Y. Xiao, "Training behavior of deep neural network in frequency domain," *NEURAL INFORMATION PROCESSING (ICONIP 2019), PT I*, pp. 264–274, 2019.
- [42] H. Wang, X. Wu, Z. Huang, and P. E. Xing, "High-frequency component helps explain the generalization of convolutional neural networks," *CVPR*, pp. 8681–8691, 2020.
- [43] S. Bubeck and M. Sellke, "A universal law of robustness via isoperimetry," in *NeurIPS 2021*, December 2021. [Online]. Available: <https://www.microsoft.com/en-us/research/publication/a-universal-law-of-robustness-via-isoperimetry/>